

# Quenching of resonance production in heavy-ion collisions

## at $1 \div 2 \text{ A GeV}$ \*

A.B. Larionov <sup>†</sup>, W. Cassing, S. Leupold, U. Mosel

*Institut für Theoretische Physik, Universität Giessen, D-35392 Giessen, Germany*

### Abstract

We study the pion production in heavy-ion collisions at SIS energies within the coupled resonance BUU model. The standard calculation overpredicts the pion multiplicity in the central Au+Au collision at 1 A GeV by about a factor of 2, which is interpreted as a signature for the quenching of the resonance production/absorption in nucleon-nucleon collisions at high nuclear density. Results of the calculations taking into account a specific form of quenching are presented for pion spectra from light and heavy systems as well as for the pion in-plane and out-of-plane flow.

### I. INTRODUCTION

Modifications of hadrons in dense nuclear matter are currently in the center of theoretical studies [1,2]. In particular, the multiple pion production in heavy-ion collisions offers an interesting possibility to look at the properties of the baryon resonances in nuclear matter [3–11]. It is well established (c.f. [3,4]) that at beam energies of  $1 \div 2 \text{ A GeV}$  pions are produced mostly in the two-step process  $NN \rightarrow NR, R \rightarrow N\pi$ , where  $R$  stands for the  $\Delta(1232)$  or higher baryon resonances. However, there is an overall tendency of transport

---

\*Supported by GSI Darmstadt

<sup>†</sup>On leave from RRC ”I.V. Kurchatov Institute”, 123182 Moscow, Russia

models explicitly propagating resonances to overpredict the pion multiplicity in heavy-ion collisions at the beam energy  $\sim 1$  A GeV (c.f. [12]). Furthermore, taking into account in-medium pion dispersion relations even increases the pion yield [13–15].

In the present work we study the effect of possible in-medium modifications of the reaction rates

$$NN \leftrightarrow NR , \quad (1)$$

on pion production. A description of the experimental data on the pion multiplicities requires an *in-medium reduction* of the rates (1). We propose, therefore, a density-dependent modification of the transition rates (1), which gives a reasonable description of the pion multiplicities in the systems C+C, Ni+Ni and Au+Au at the beam energy of 1÷2 A GeV. We will show, moreover, that this modification is consistent with other pion observables, i.e. transverse mass and kinetic energy spectra, angular distributions and in-plane collective flow.

The structure of the paper is as follows: In Sect. II we discuss the effect of the resonance production/absorption quenching on the pion production. Sect. III contains the results on the collective pion flows, while in Sect. IV the summary and conclusions are given.

## II. DENSITY DEPENDENT TRANSITION RATES $NN \leftrightarrow NR$

In our numerical calculations we have used the BUU model in the version described in Ref. [16]. The nucleons,  $\Delta(1232)$  and higher (up to  $D_{35}(2350)$ ) baryon resonances,  $\Lambda$  and  $\Sigma$  hyperons, mesons  $\pi$ ,  $\eta$ ,  $\omega$ ,  $K$ ,  $\rho$ ,  $\sigma$  are explicitly propagated in this BUU implementation. The model has been successfully applied to the calculation of nucleon collective flow observables in heavy-ion collisions at energies from  $\sim 100$  AMeV up to  $\sim 2$  A GeV [17]. A good description of "more elementary"  $\gamma$  and  $e^-$  induced reactions has been also reached within the model (see Refs. [16,18]).

In this work we concentrate on pion production in nucleus-nucleus collisions continuing the studies initiated in Refs. [6,11]. All calculations in the present paper are performed using

the soft momentum-dependent mean field (SM) with incompressibility  $K = 220$  MeV, which gives the best overall description of the nucleon collective flow variables [17]. The BUU set of parameters, which includes the SM mean field as well as vacuum resonance parameters and vacuum elastic and inelastic cross sections, will be denoted as "standard" below. The modifications of the standard set will be discussed in the text explicitly.

First, we compare the calculated pion multiplicities in central Au+Au collisions at 1 A GeV with the experimental data. In Fig. 1 the dashed line shows the pion number vs time in the case of the standard calculation. The pion multiplicity asymptotically reaches a value of  $\sim 60$  which is almost a factor of 2 larger than the experimental value of  $\sim 34$  (c.f. Ref. [12]). Pions are produced dominantly by the baryon resonance decays. Therefore, the pion multiplicity is very sensitive to the number of resonances present in the system. The differential production cross section of a resonance  $R$  with mass  $M$  in a nucleon-nucleon collision, averaged over the spins of initial particles and summed over the spins of final particles, is given as

$$\frac{d\sigma_{N_1 N_2 \rightarrow N_3 R_4}}{dM^2 d\Omega} = \frac{1}{64\pi^2} \overline{|\mathcal{M}|^2} \frac{p_{34}}{p_{12}\varepsilon^2} \mathcal{A}(M^2) \times 2(2J_R + 1) , \quad (2)$$

where  $\overline{|\mathcal{M}|^2}$  is a spin-averaged matrix element squared,  $p_{12}$  and  $p_{34}$  are c.m. momenta of incoming and outgoing particles,  $\varepsilon$  is the total c.m. energy,  $\mathcal{A}(M^2)$  is the spectral function of the resonance, and  $J_R$  is the spin of the resonance. The inverse reaction cross section is

$$\frac{d\sigma_{N_3 R_4 \rightarrow N_1 N_2}}{d\Omega} = \frac{1}{64\pi^2} \overline{|\mathcal{M}|^2} \frac{p_{12}}{p_{34}\varepsilon^2} \times \frac{4}{C_{12}} , \quad (3)$$

where, due to detailed balance, the same matrix element appears as in Eq. (2),  $C_{12} = 2$  if the nucleons  $N_1$  and  $N_2$  are identical and  $C_{12} = 1$  otherwise.

The matrix element which appears in Eqs. (2),(3) should be evaluated in nuclear matter. Instead of using any model dependent parametrizations for the in-medium matrix element, we adopt a simple relation

$$\overline{|\mathcal{M}|^2} = \kappa(\rho) \overline{|\mathcal{M}_{vac}|^2} , \quad \kappa(0) = 1 , \quad (4)$$

where  $|\mathcal{M}_{vac}|^2$  is the vacuum matrix element squared and  $\kappa(\rho)$  is some density-dependent function to be determined by comparison with the experimental data. The in-medium matrix elements for the non-resonant (background) one-pion production/absorption  $N_1 N_2 \leftrightarrow N_3 N_4 \pi$ , double  $\Delta(1232)$  production/absorption  $N_1 N_2 \leftrightarrow \Delta_3 \Delta_4$  and resonance scattering on nucleons  $N_1 R_2 \rightarrow N_3 R_4$  are also related to their vacuum values by Eq. (4) with the same universal function  $\kappa(\rho)$ .

We address now the pion multiplicity in central Au+Au collisions at 1.06 A GeV using various choices of the function  $\kappa(\rho)$ . As a first trial, we simulate an enhancement of resonance production in NN collisions [19] assuming a linear dependence on density as in Refs. [11,20]:

$$\kappa(\rho) = 1 + \beta \frac{\rho}{\rho_0} , \quad \beta > 0 , \quad (5)$$

where  $\rho_0 = 0.16 \text{ fm}^{-3}$  is the equilibrium nuclear matter density. We see from Fig. 1 (dotted line), that the amplified matrix element with  $\kappa(\rho) = 1 + 3\rho/\rho_0$  leads to an about 20% reduction in the final pion multiplicity which, however, is still above the experimental abundance. This decrease originates from the amplified – by detailed balance – absorption of resonances in the expansion stage of the system. A further increase of the parameter  $\beta$  practically does not reduce the pion number any further (see Fig. 3 for  $\beta > 0$ ).

An essential reduction of the pion multiplicity can only be reached by a *quenching* of the resonance production/absorption processes in nuclear matter at high density. To this aim we apply a piece-wise linear function of the form

$$\kappa(\rho) = \min(1, \max(0, 1 + \beta(\rho/\rho_0 - 1))) , \quad \beta < 0 , \quad (6)$$

which is shown by the solid line in Fig. 2 for the particular case  $\beta = -2$ . Within the parametrization (6), the in-medium effects vanish at subnuclear densities ( $\kappa = 1$ ), but above  $\rho_0$  the nuclear medium creates the shadowing of binary collisions involving resonances leading, effectively, to a quenching of these collisions for  $\rho \geq (1 - 1/\beta)\rho_0$ . In Fig. 3 (see the part of the BUU curve for  $\beta < 0$ ) we report the number of produced negative pions vs  $\beta$  in the case of the parametrization (6). The proper pion multiplicity is reproduced for  $\beta = -2$ ; we

will denote this calculation as “quenched” in the following. For this calculation, resonances do not experience any elastic or inelastic scatterings in high density nuclear matter. They can, however, decay or be produced in the processes  $R \leftrightarrow N\pi$ . In the quenching scenario, the resonance production in NN collisions happens only at relatively low density  $\rho \leq 1.5\rho_0$ , i.e. dominantly in the overlapping tails of the density profiles of colliding nuclei. This reduces the maximum number of  $\Delta$ -resonances to about 35% as compared to a standard calculation (c.f. solid and dashed lines in the lower panel of Fig. 1).

Before discussing other pion-related observables we check, how the resonance quenching influences the underlying nucleon dynamics. Fig. 4 shows the proton rapidity distribution and the transverse momentum of protons in the reaction plane as a function of rapidity. Due a lower nucleon inelasticity within the quenching scenario, the nuclei show less stopping, i.e. the rapidity distribution becomes somewhat wider and, since also the pressure is decreased, a slightly smaller transverse in-plane flow is generated making the agreement of the standard SM calculation [17] with the proton flow data worse (see also Fig. 11). This problem, however, can be resolved by either increasing the incompressibility or the stiffness of the momentum-dependent interaction. The latter modifications influence only weakly the pion multiplicity and, therefore, are not studied in this work.

In Fig. 5 we present the pion multiplicity as a function of the participant number  $A_{part}$  for Au+Au collisions at 1.06 A GeV in comparison with the FOPI and TAPS data collected in Ref. [12]. We have determined the participant number for a given impact parameter using the participant-spectator model with sharp nuclear density profiles. The quenched calculation is in a good agreement with the data for central collisions; in peripheral collisions the medium effects are smaller, the difference between the standard and the quenched calculation vanishes gradually and, thus, the multiplicity is still somewhat overpredicted. This discrepancy in peripheral collisions could arise from different definitions of the participant number  $A_{part}$  in our calculations and in Ref. [12], since the impact parameter can not be measured directly in the experiment.

Fig. 6 shows the beam energy dependence of the charged pion multiplicity for central

Ni+Ni collisions compared with the FOPI data from Ref. [21]. The quenched calculation describes the data rather well. With increasing beam energy the difference between standard and quenched calculations reduces, since the nonresonant string mechanism for pion production becomes dominant, which is the same in both calculations. We recall that in our transport approach strings are excited in NN collisions for invariant collision energies  $\sqrt{s} \geq 2.6$  GeV corresponding to the beam energy of 1.73 A GeV if the Fermi motion is neglected.

Fig. 7 shows the c.m. kinetic energy spectra of charged pions at  $\Theta_{c.m.} = 130^\circ$  for Au+Au at 1.06 A GeV. The quenching again improves the agreement with the data producing a more concave shape of the spectrum for  $E_{kin}^{c.m.} > 0.1$  GeV. At lower pion energies, however, the data are slightly underestimated in the quenched calculation.

A similar tendency is visible in the case of  $p_t$ -spectra shown in Fig. 8: the improvement by the quenching mechanism at high  $p_t$  is evident, but at low  $p_t$  too few pions are produced. The reason is, probably, an overdamping of the low mass resonance production in NN collisions at high density by the quenching factor (6). Indeed, a smaller medium effect is expected for higher kinetic energies of final particles in analogy to Pauli blocking [23]. In this exploratory work we are not aiming to get a detailed description of the pion energy spectra, but, rather, to demonstrate the gross effect of the density modified matrix element on various pion observables. It is straightforward, however, to introduce a  $\sqrt{s}$  and resonance-mass-dependent modification factor  $\kappa$  in Eq.(4).

In Fig. 9 we present the c.m. polar angle distributions of charged pions. The shape of these spectra is similar to the one for free-space pion production in NN collisions. There is a good overall agreement of the quenched calculation with the data.

For the collisions C+C at 0.8÷2 A GeV (Fig. 10) the calculated  $m_t$ -spectra of  $\pi^0$ 's are practically identical in the standard and quenched calculations. This is expected, since the in-medium modifications are smaller in the lighter system.

### III. COLLECTIVE FLOW

In earlier studies (c.f. [4,25]), the pion antiflow and squeeze-out have been explained by the rescattering of pions on the spectator nucleons, which leads to the shadowing phenomenon.

Fig. 11 shows the proton,  $\pi^+$  and  $\pi^-$  in-plane flow ( $:= d < p_x > /dY^{(0)}$  at  $Y^{(0)} = 0$ ) for the Au+Au system at 1.15 A GeV as a function of impact parameter in comparison to the data [26]. The best overall agreement with the data is reached within the standard SM calculation. For  $\pi^\pm$ , the quenched and standard results are almost indistinguishable within statistics. However, the proton flow is underpredicted by the quenched calculation (see discussion in the previous section). The difference in flows for  $\pi^+$  and  $\pi^-$  is due to the Coulomb interaction with protons which increases (decreases) the antiflow for  $\pi^+$  ( $\pi^-$ ) for large impact parameter.

In Fig. 12 we show the squeeze-out ratio  $R_N := (N_{\pi^+}(90^\circ) + N_{\pi^+}(-90^\circ))/(N_{\pi^+}(0^\circ) + N_{\pi^+}(180^\circ))$  as a function of the transverse momentum for positive pions at midrapidity in comparison to the data [27]. The squeeze-out ratio grows with  $p_t$  since faster moving pions in transverse direction reach the spectators earlier and rescatter in analogy to the case of the nucleon squeeze-out [17]. A peculiar feature of the  $R_N(p_t)$ -dependence for positive pions is its saturation at relatively low  $p_t \sim 0.3$  GeV/c, while the nucleon squeeze-out ratios increase monotonically with  $p_t$  (c.f. [28,29]). This behaviour of the pion squeeze-out ratio is related to the resonance nature of  $\pi N$  scattering [25]. Our calculations, both standard and quenched, underpredict the absolute value of  $R_N$ , but the shape of the function  $R_N(p_t)$  is in a qualitative agreement with the data. The reason for this discrepancy lies, most probably, in the absence of any momentum dependence in the pion potential. The ratio  $R_N$  is influenced also by the modifications of the resonance life times [30].

#### IV. SUMMARY AND CONCLUSIONS

Within the transport BUU model [16] we have studied the influence of the in-medium modifications of the reaction rates (1) on pion production in heavy-ion collisions around 1 A GeV. The pion multiplicity in the system Au+Au at 1 A GeV can be consistently described assuming a quenching of the resonance production/absorption in NN collisions at high nuclear densities. The quenching generally improves the description of standard BUU calculations with experiment on other pion observables:  $p_{t-}$ ,  $m_{t-}$  and kinetic energy spectra, in-plane and out-of-plane collective flows.

The physical reason for the in-medium reduction of the resonance production rates, that seems to be needed to describe the pion data, remains open. This is in particular so because there are theoretical predictions that the  $\Delta$  excitation cross section should increase with density [19]. A collisional broadening of the  $\Delta$ -resonance, that was not taken into account in Ref. [19], could, in principle, provide the obviously needed reduction, but the calculations of Ref. [31], that were based on reasonable collision rates, have shown that this broadening is too small. All these models have in common that they work with free coupling constants and thus neglect any in-medium vertex corrections. Good calculations of inelastic nucleon-nucleon scattering in nuclear matter would be needed to clarify this problem.

## REFERENCES

- [1] C.M. Ko, V. Koch, and G.Q. Li, Ann. Rev. Nucl. Part. Sci. **47**, 505 (1997).
- [2] W. Cassing and E.L. Bratkovskaya, Phys. Rep. **308**, 65 (1999).
- [3] W. Ehehalt, W. Cassing, A. Engel, U. Mosel, and Gy. Wolf, Phys. Rev. C **47**, R2467 (1993).
- [4] S.A. Bass, C. Hartnack, H. Stöcker, and W. Greiner, Phys. Rev. C **51**, 3343 (1995).
- [5] C.M. Ko and G.Q. Li, J. Phys. G **22**, 1673 (1996).
- [6] S. Teis, W. Cassing, M. Effenberger, A. Hombach, U. Mosel and Gy. Wolf, Z. Phys. A **356**, 421 (1997).
- [7] E.L. Hjort et al., Phys. Rev. Lett. **79**, 4345 (1997).
- [8] W. Weinhold, B. Friman and W. Nörenberg, Phys. Lett. B **433**, 236 (1998).
- [9] M. Eskef et al., Eur. Phys. J. A **3**, 335 (1998).
- [10] D. Pelte, nucl-ex/9902006.
- [11] A.B. Larionov, A. Cassing, M. Effenberger, U. Mosel, Eur. Phys. J. A **7**, 507 (2000).
- [12] D. Pelte et al., Z. Phys. A **357**, 215 (1997).
- [13] W. Ehehalt et al., Phys. Lett. B **298**, 31 (1993).
- [14] J. Helgesson and J. Randrup, Phys. Lett. B **411**, 1 (1997).
- [15] J. Helgesson and J. Randrup, Phys. Lett. B **439**, 243 (1998).
- [16] M. Effenberger, E.L. Bratkovskaya, and U. Mosel, Phys. Rev. C **60**, 044614 (1999).
- [17] A.B. Larionov, W. Cassing, C. Greiner, and U. Mosel, Phys. Rev. C **62**, 064611 (2000).
- [18] J. Lehr, M. Effenberger and U. Mosel, Nucl. Phys. A **671**, 503 (2000).

[19] G.F. Bertsch, G.E. Brown, V. Koch and B.A. Li, Nucl. Phys. A **490**, 745 (1988).

[20] A. Engel, W. Cassing, U. Mosel, M. Schäfer and Gy. Wolf, Nucl. Phys. A **572**, 657 (1994).

[21] D. Pelte et al., Z. Phys. A **359**, 55 (1997).

[22] O. Schwalb et al., Phys. Lett. B **321**, 20 (1994).

[23] To avoid misunderstanding, we note, that usual Pauli blocking for nucleons in final states is always included for both standard and quenched calculations.

[24] R. Averbeck et al., Z. Phys. A **359**, 65 (1997).

[25] Bao-An Li, Nucl. Phys. A **570**, 797 (1994).

[26] J.C. Kintner et al., Phys. Rev. Lett. **78**, 4165 (1997).

[27] Y. Shin et al., Phys. Rev. Lett. **81**, 1576 (1998).

[28] D. Lambrecht et al., Z. Phys. A **350**, 115 (1994).

[29] D. Brill et al., Z. Phys. A **355**, 61 (1996).

[30] A.B. Larionov, S. Leupold, U. Mosel, in preparation.

[31] M. Effenberger, A. Hombach, S. Teis, U. Mosel, Nucl. Phys. A **613**, 353 (1997).

## FIGURE CAPTIONS

**Fig. 1** Pion number (upper panel) and  $\Delta$ -resonance number (lower panel) vs time for a central collision Au+Au at 1.06 A GeV. Standard calculations are represented by dashed lines. The dash-dotted and dotted lines show the cases of in-medium amplified reaction rates (1) for  $\beta = 1$  and  $\beta = 3$ , respectively, while the solid lines correspond to the quenched calculation ( $\beta = -2$ ). The experimental data from Ref. [12] are within the dashed band in the upper panel.

**Fig. 2** Density dependence of the modification factor  $\kappa(\rho)$  of the matrix element for resonance production/absorption (see Eq.(4)). The notation of lines is the same as in Fig. 1.

**Fig. 3** Number of negative pions for the central collision Au+Au at 1.06 A GeV as a function of the coefficient  $\beta$  in the density dependence of the factor  $\kappa$  (see Eqs.(5),(6)). The part at  $\beta < 0$  corresponds to the parametrization (6), while  $\kappa(\rho) = 1 + \beta\rho/\rho_0$  for  $\beta > 0$ . The dashed band represents the experimental data from Ref. [12].

**Fig. 4** Proton rapidity distribution (upper panel) and rapidity dependence of the proton transverse momentum in the reaction plane (lower panel) for Au+Au collision at 1.06 A GeV and impact parameter  $b=6$  fm. The rapidity is normalized to the projectile rapidity in the center-of-mass system:  $Y^{(0)} \equiv (y/y_{proj})_{c.m.}$ .

**Fig. 5**  $\pi^-$ ,  $\pi^0$  and  $\pi^+$  multiplicities (left, central and right panels, respectively) vs participant number  $A_{part}$  for the system Au+Au at 1.06 A GeV. The experimental data are from Ref. [12].

**Fig. 6**  $\pi^-$  and  $\pi^+$  multiplicities (left and right panels, respectively) in central collisions of Ni+Ni as a function of the beam energy. The BUU calculations are performed for  $b=1$  fm. The experimental data are from Ref. [21].

**Fig. 7** C.m. kinetic energy spectra of negative and positive pions (upper and lower panels, respectively) at  $\Theta_{c.m.} = 130^\circ$  for Au+Au at 1.06 A GeV. The experimental data are from Ref. [12].

**Fig. 8**  $\pi^-$ ,  $\pi^0$  and  $\pi^+$  transverse momentum spectra at midrapidity for Au+Au at 1.06 A GeV. The spectra are calculated in the rapidity intervals  $Y^{(0)} = -0.2 \div 0.2$  for  $\pi^\pm$  and  $Y^{(0)} = -0.25 \div 0.21$  for  $\pi^0$ , but normalized to a rapidity interval  $dy = 1$  following Refs. [12,22]. The experimental data are from Refs. [12,22].

**Fig. 9** C.m. polar angle distributions of charged pions in Au+Au collisions at 1.06 A GeV. Left and right panels show, respectively, the  $\pi^-$  and  $\pi^+$  distributions for the c.m. kinetic energy  $E_{kin}^{c.m.} > 40$  MeV, while the central panel presents the  $\pi^-$  distribution for  $E_{kin}^{c.m.} > 365$  MeV. The experimental data are from Ref. [12].

**Fig. 10** Transverse mass spectra of  $\pi^0$ 's in selected rapidity intervals near midrapidity (following Ref. [24]) for C+C collisions at 0.8, 1 and 2 A GeV:  $y_{lab} = 0.42 \div 0.74$ ,  $0.42 \div 0.74$  and  $0.8 \div 1.08$ , respectively. The thick solid lines show exponential fits to the experimental data from Ref. [24].

**Fig. 11** In-plane flow as a function of impact parameter for protons (upper panel),  $\pi^+$ 's (middle panel) and  $\pi^-$ 's (lower panel) in comparison with the experimental data from Ref. [26] for Au+Au at 1.15 A GeV.

**Fig. 12** Transverse momentum dependence of the squeeze-out ratio  $R_N$  for positive pions for semicentral Au+Au collisions at 1 A GeV. The calculated results are impact-parameter-weighted in the range  $b = 5 \div 7$  fm. The experimental data are from Ref. [27].

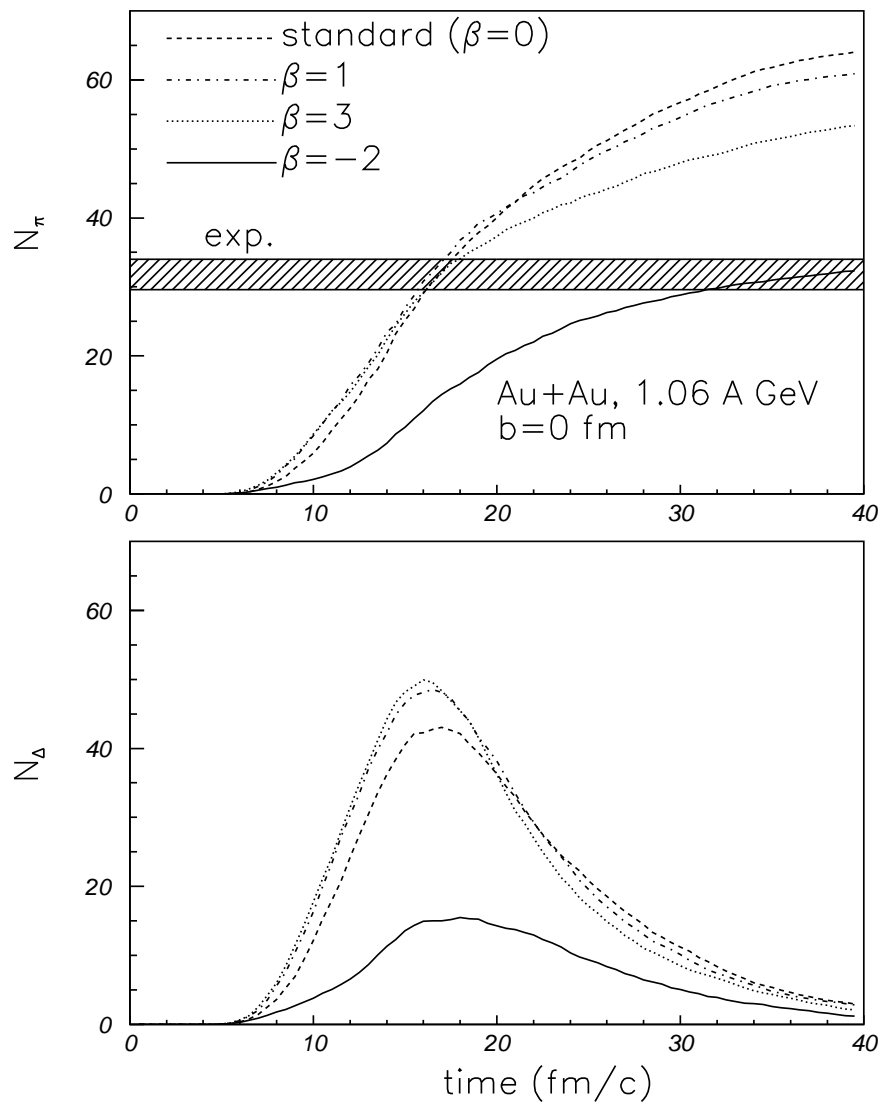


FIG. 1.

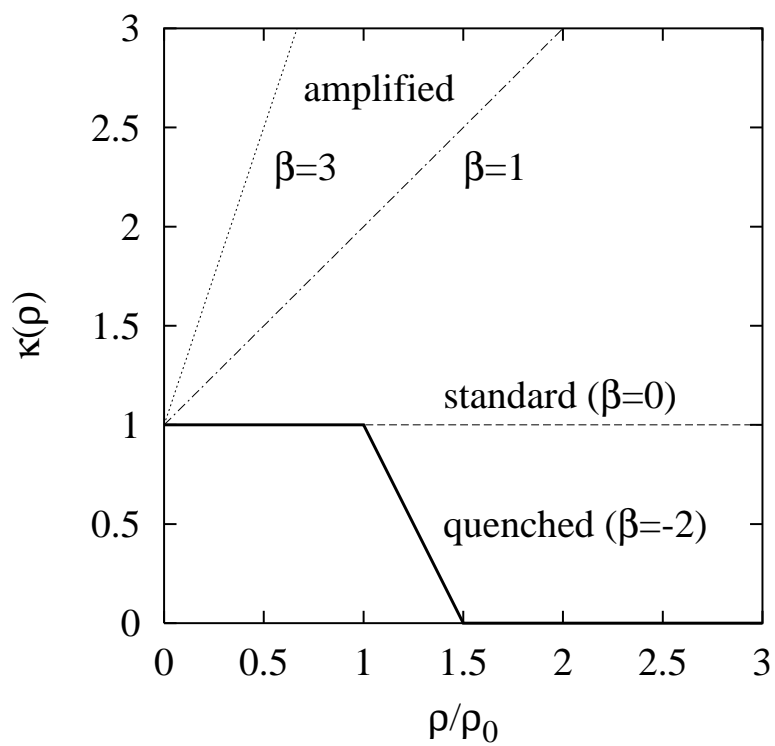


FIG. 2.

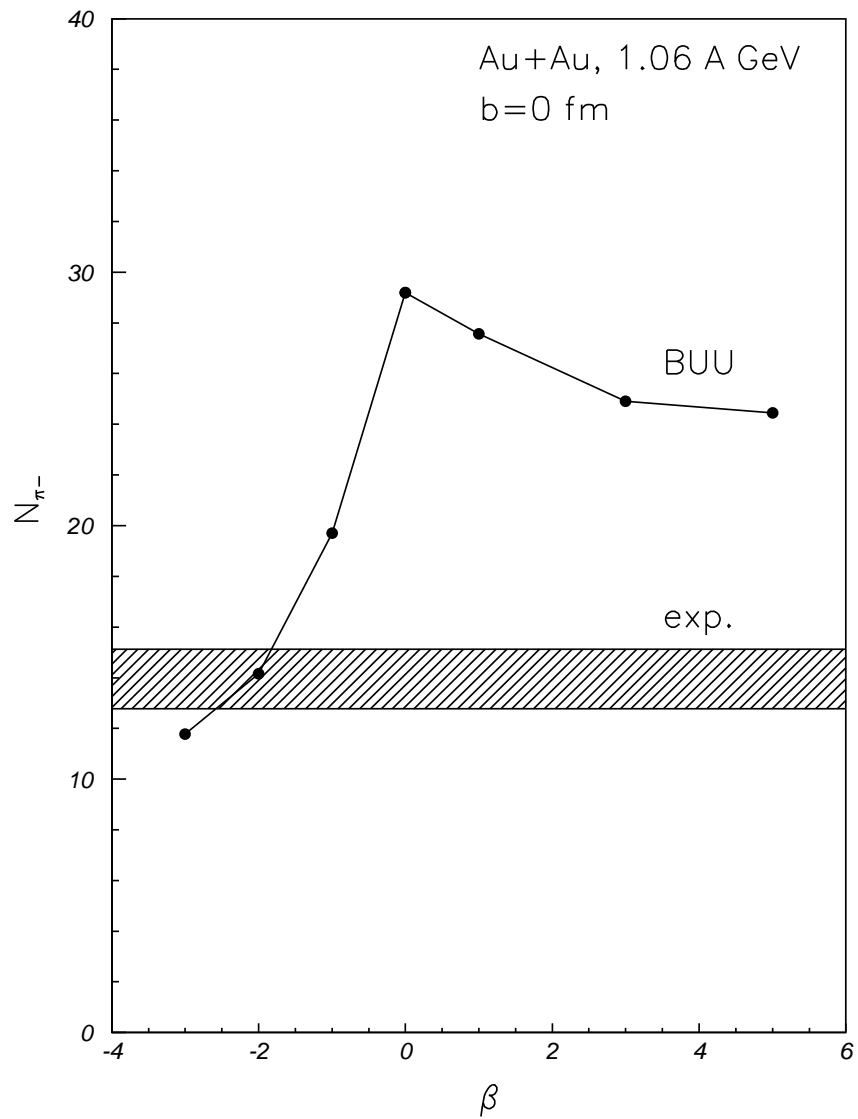


FIG. 3.

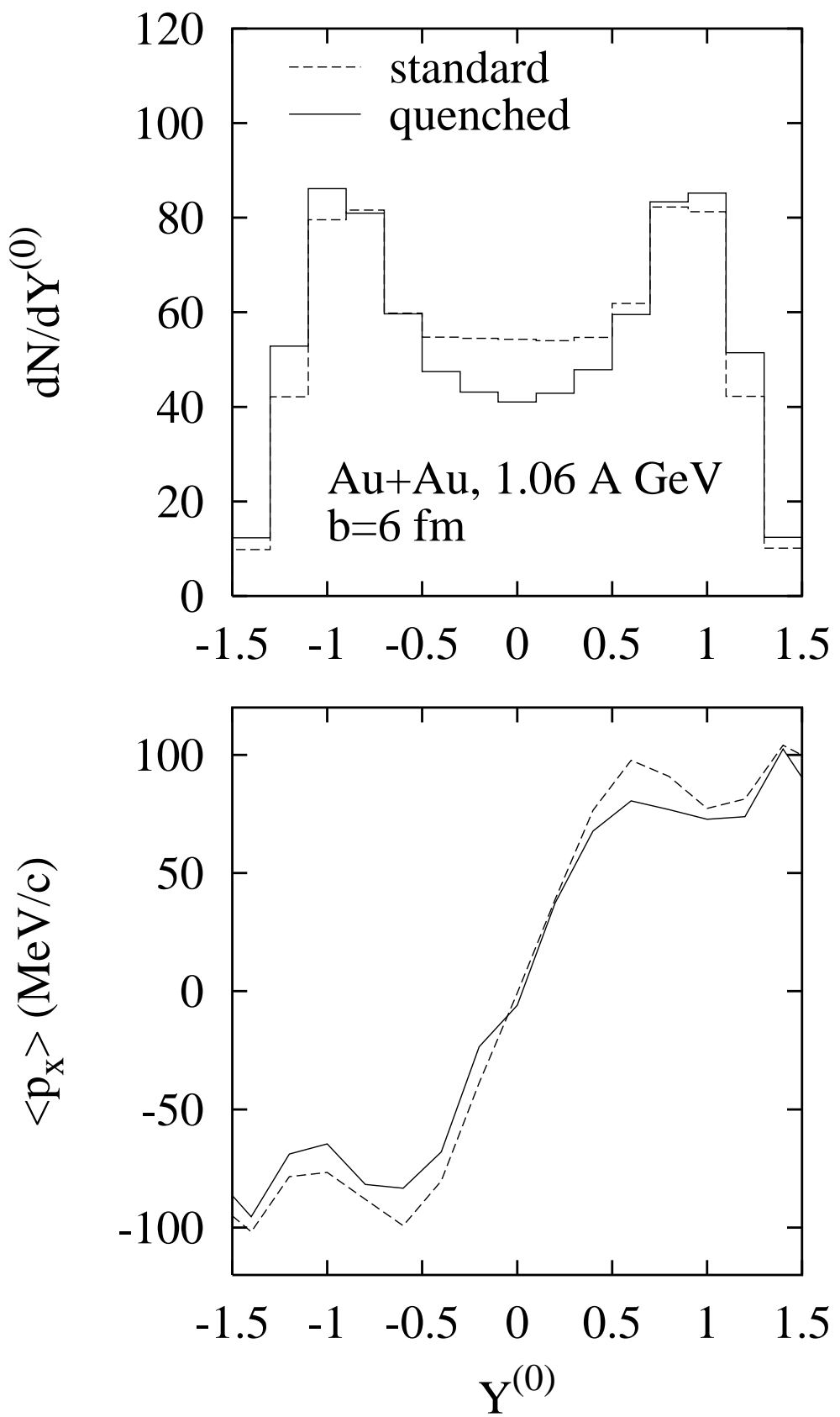


FIG. 4.

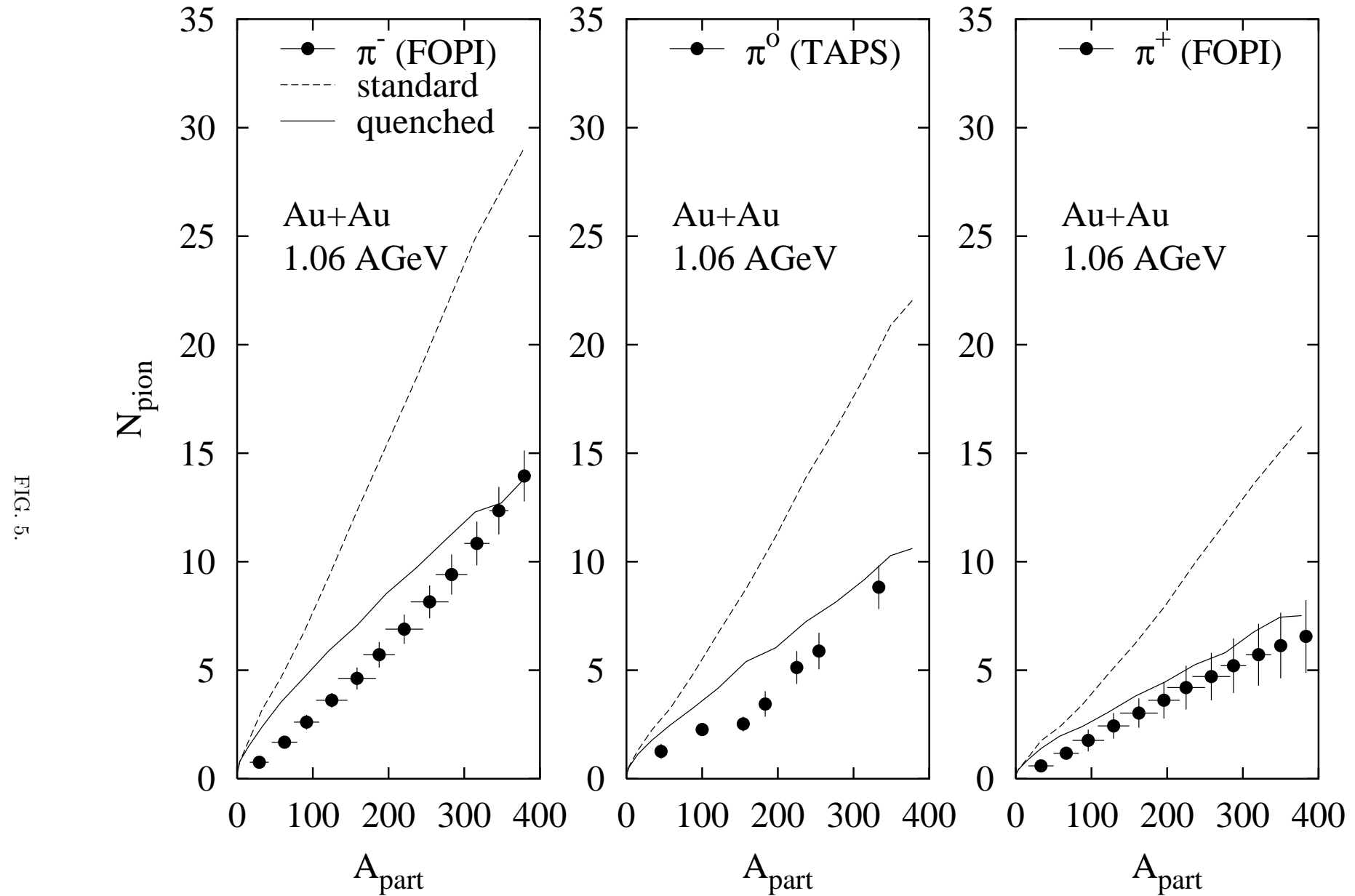
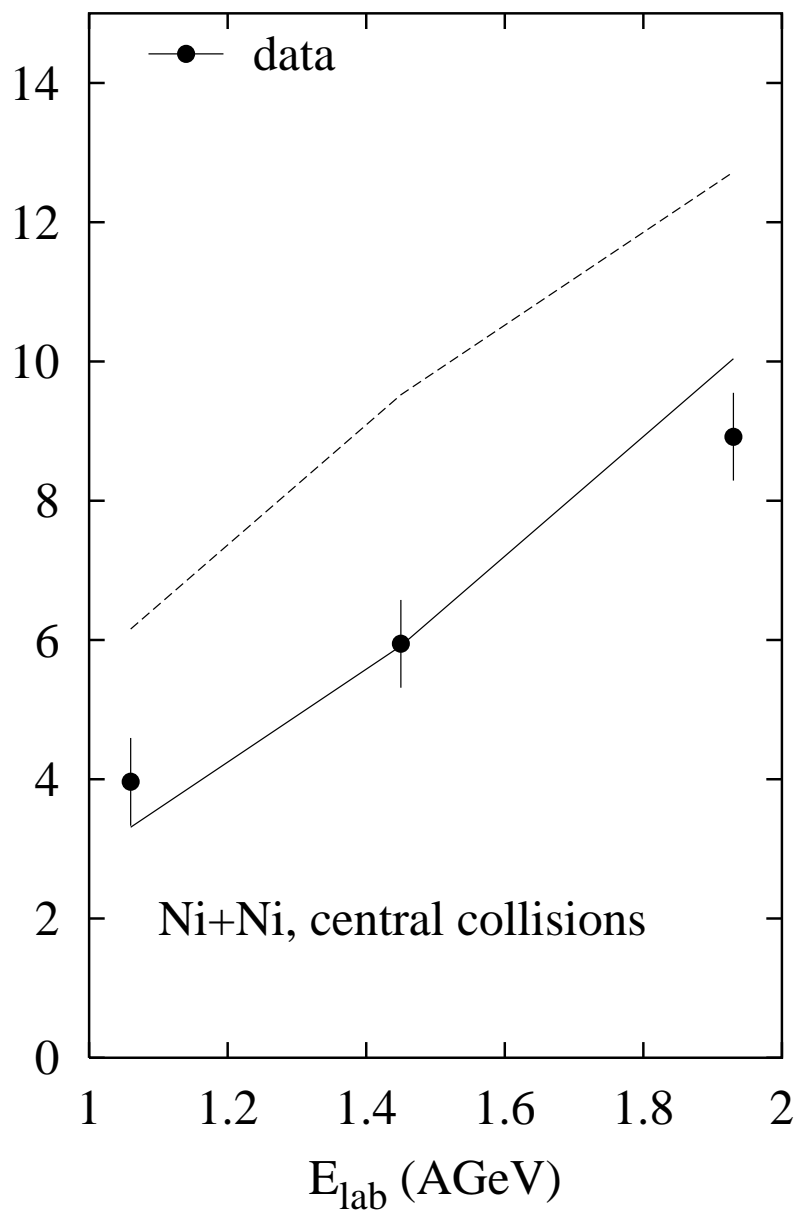
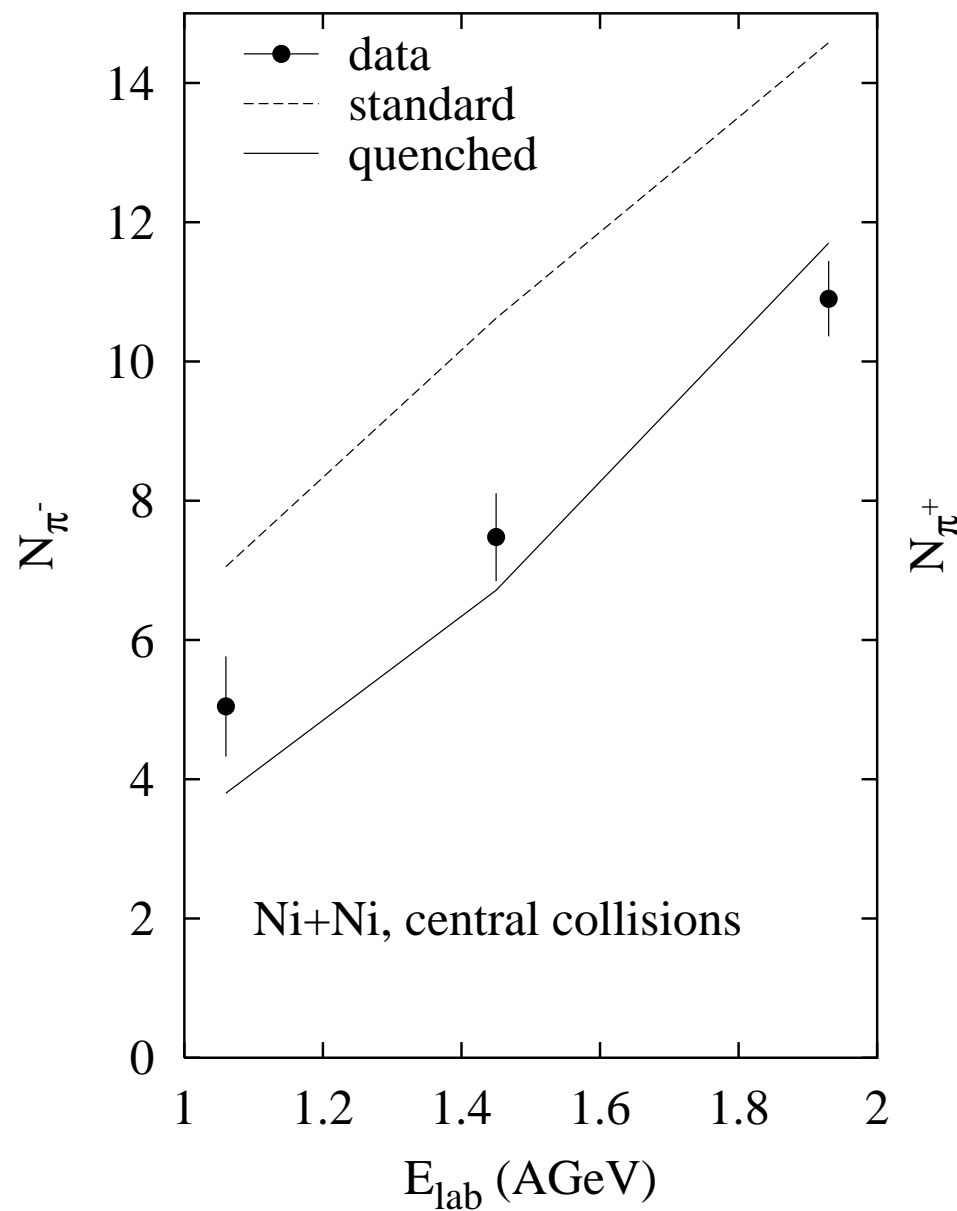


FIG. 6.



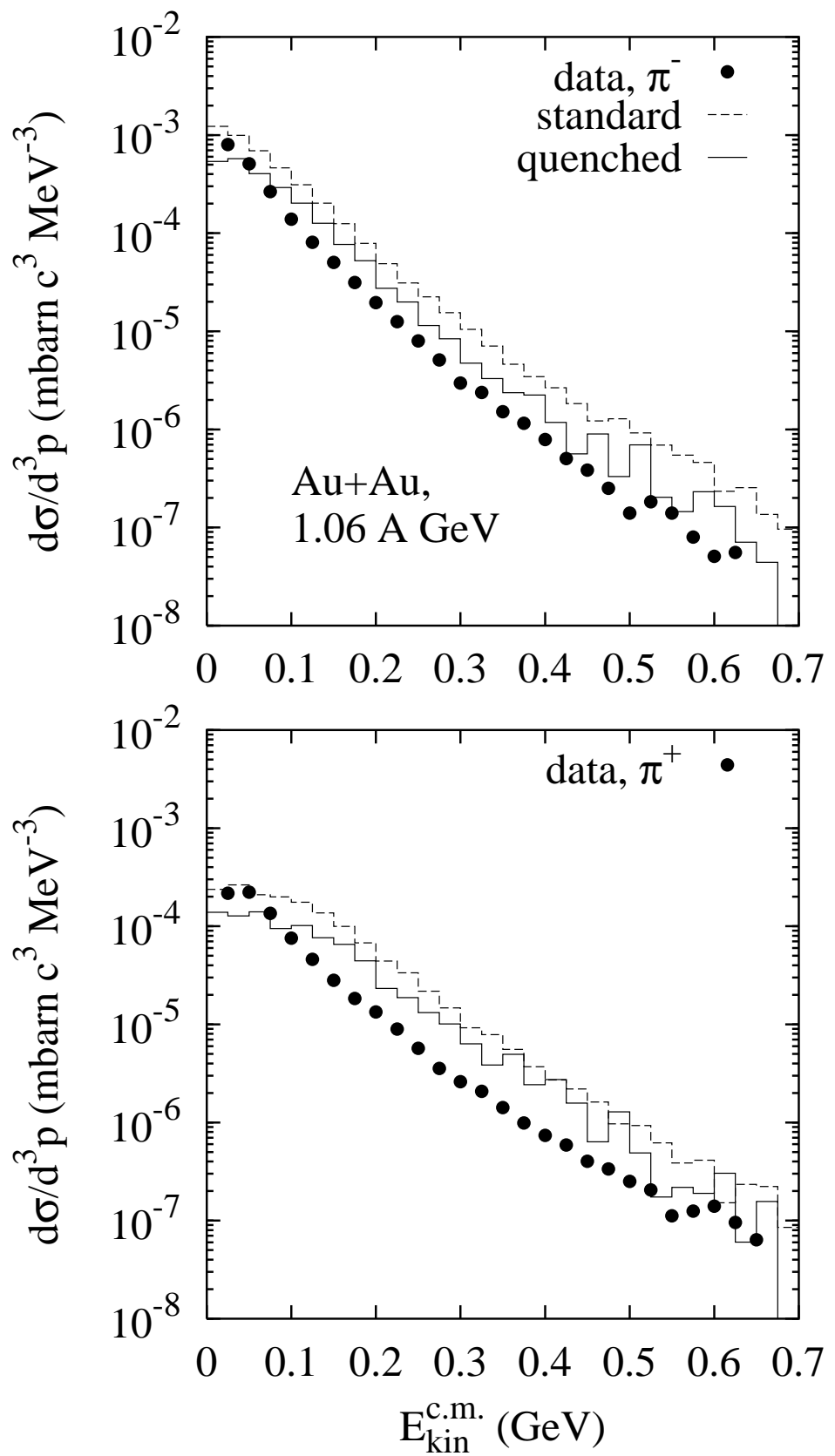


FIG. 7.

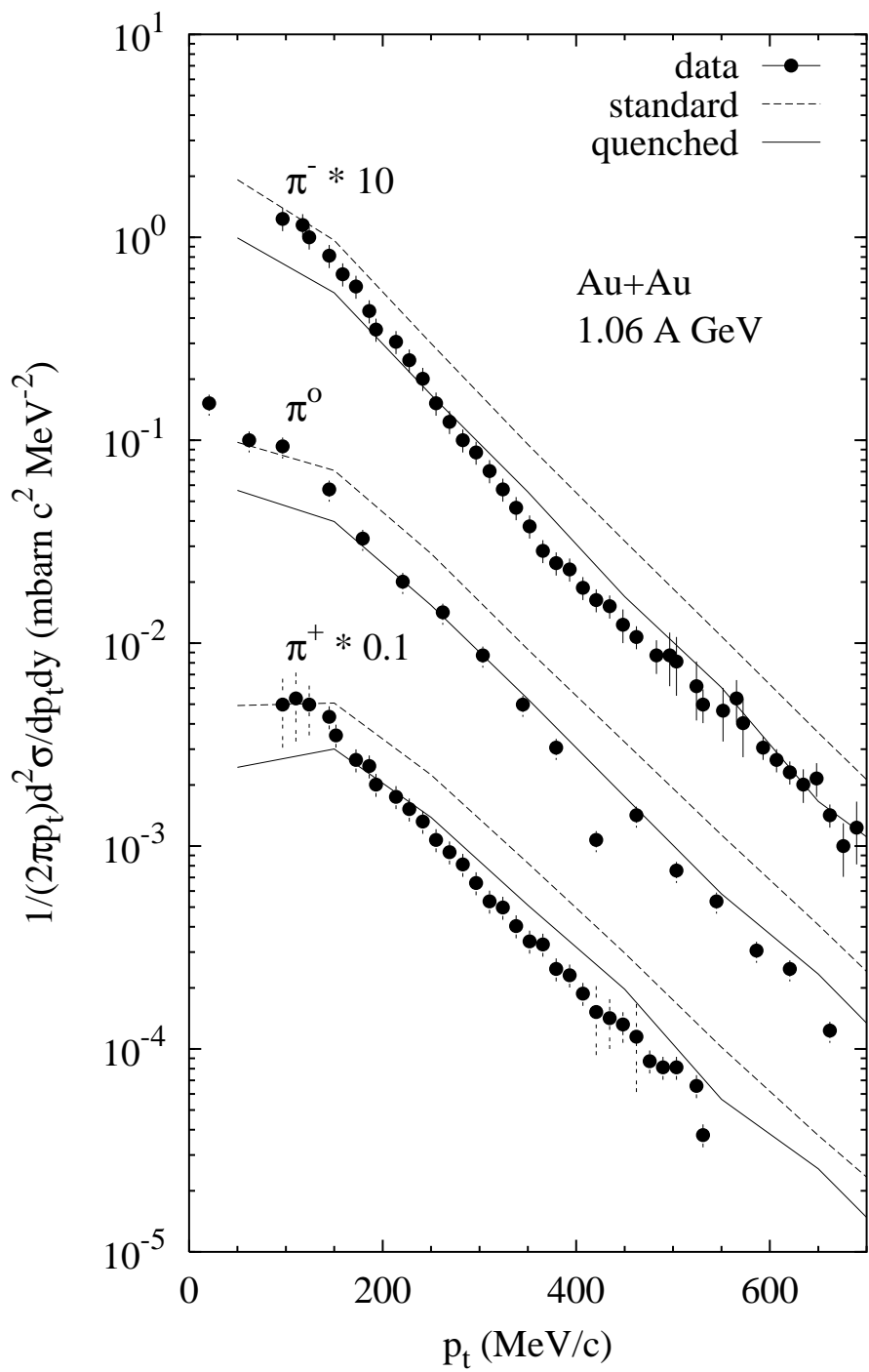
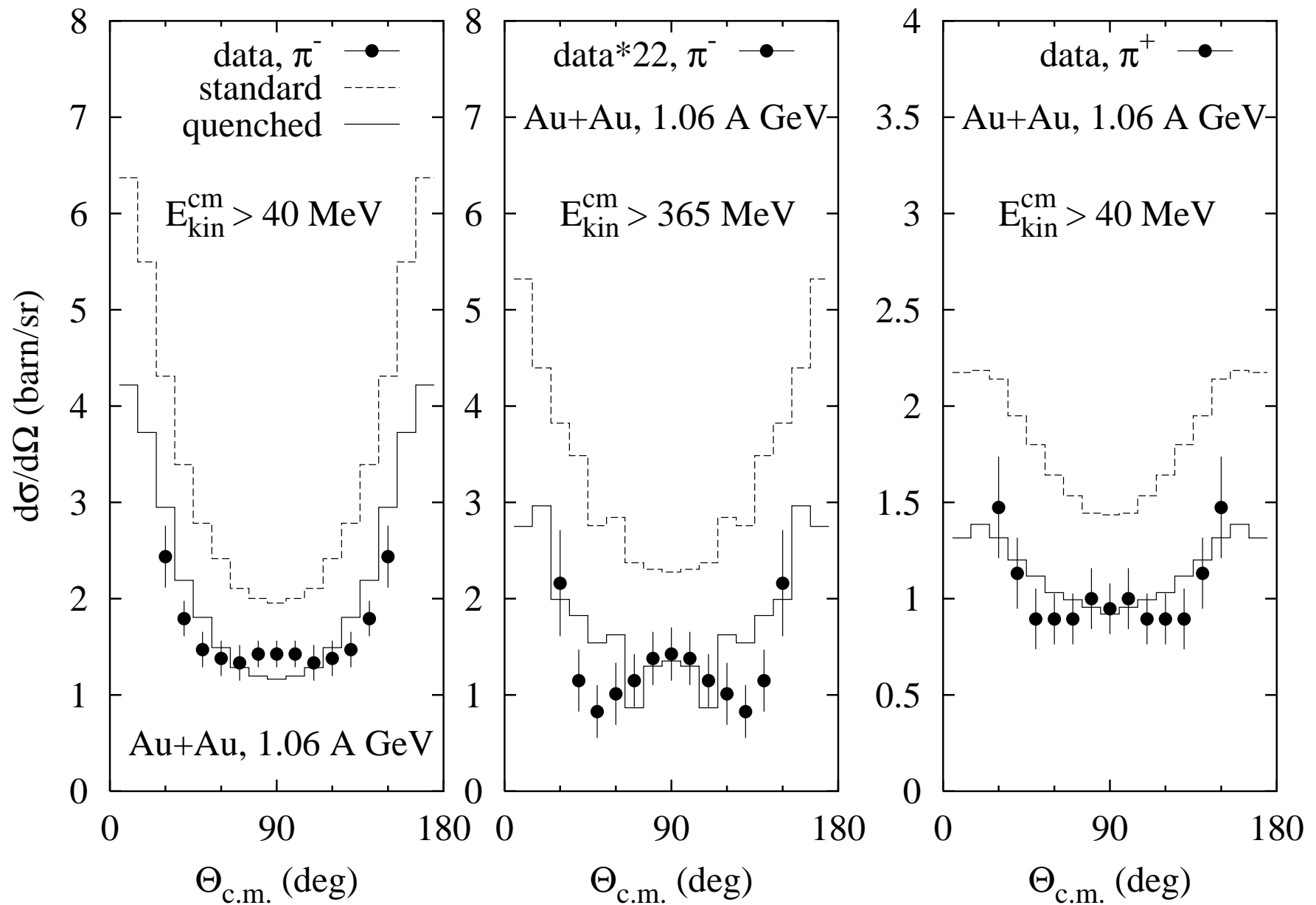


FIG. 8.

FIG. 9.



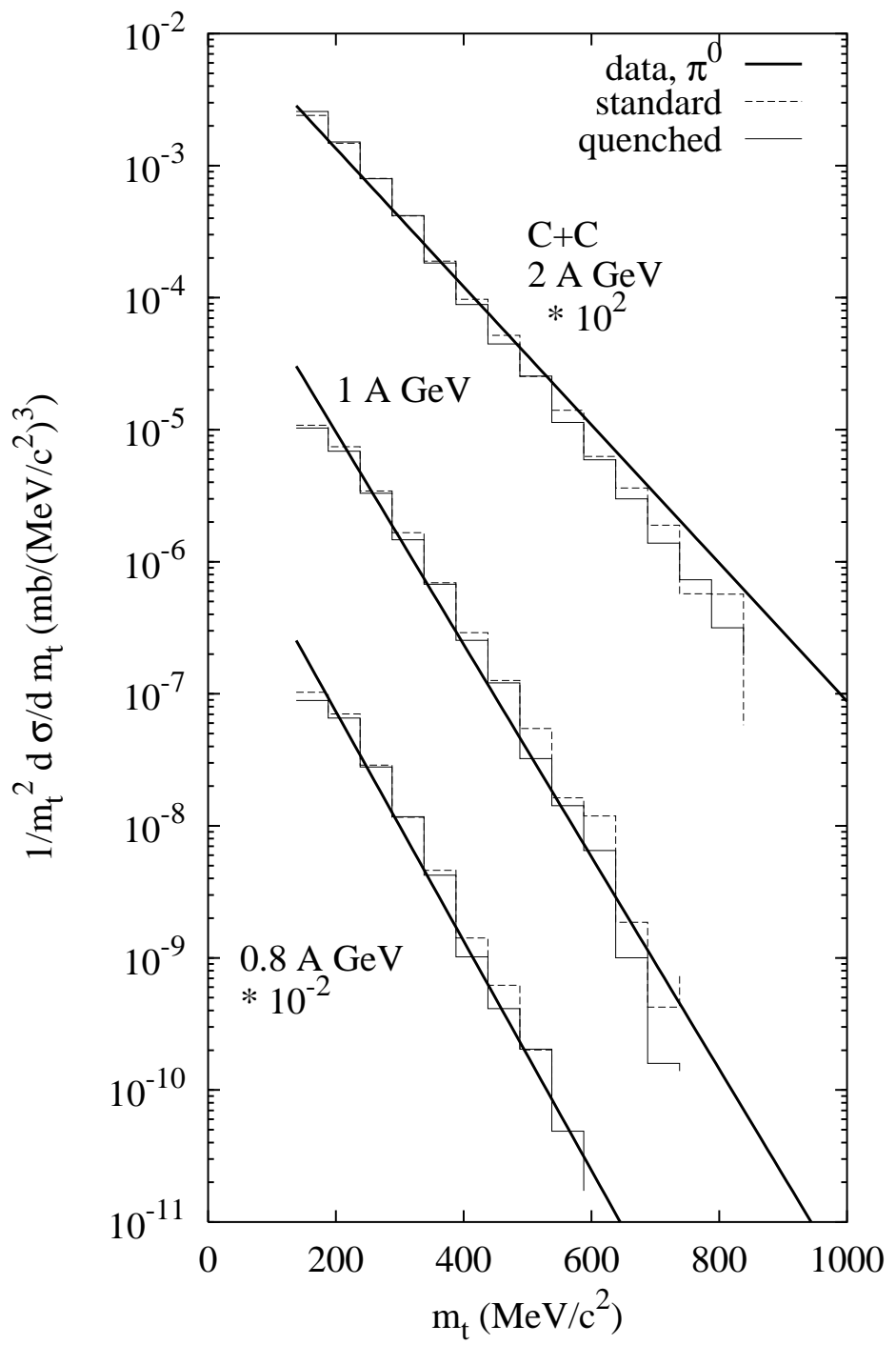


FIG. 10.

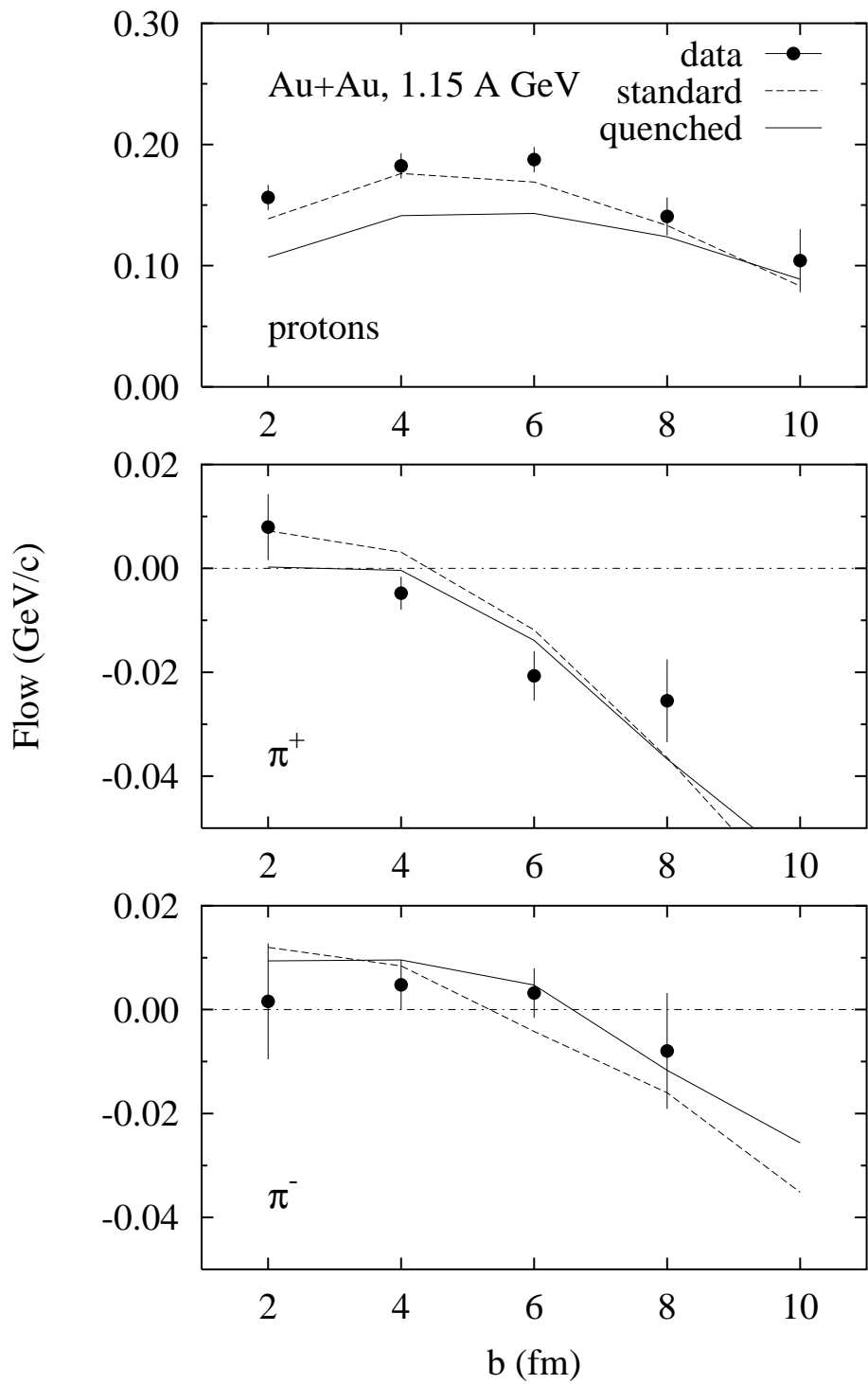


FIG. 11.

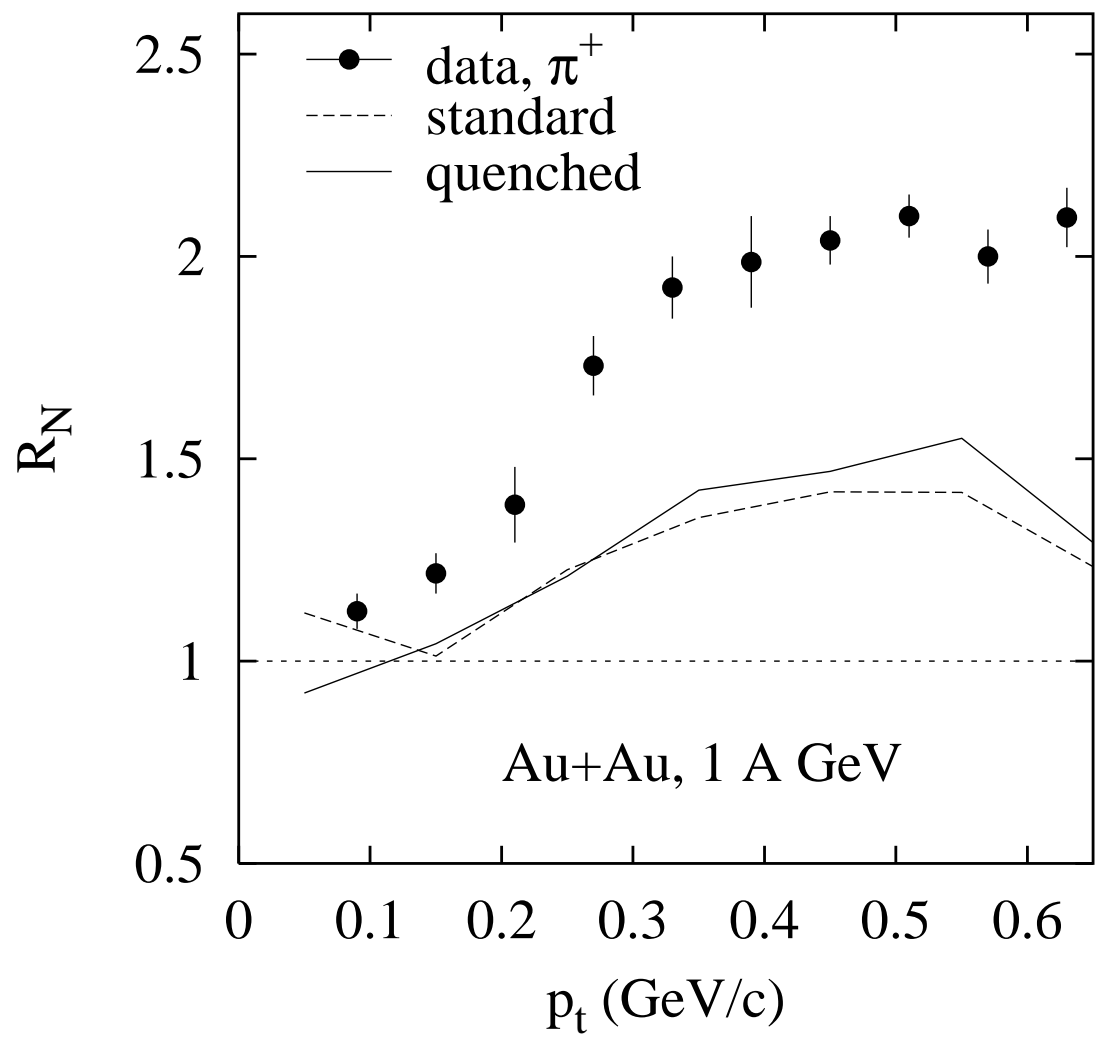


FIG. 12.